

1 **Supporting Information**

2

3 **Strain-Induced Catalytic Enhancement in Co-BTA and Rh-BTA for**
4 **Efficient 2e⁻ Oxygen Reduction: A DFT Study**

5 Ran Tao¹, Cheng Liu^{1†}, Weihua Ning^{1†}, Youyong Li^{1,2†}

6 ¹Institute of Functional Nano & Soft Materials (FUNSOM), Jiangsu Key Laboratory
7 for Carbon-Based Functional Materials and Devices, Soochow University, Suzhou
8 215123, China.

9 ²Macao Institute of Materials Science and Engineering, Macau University of Science
10 and Technology, Taipa 999078, Macau SAR, China

11

12 † Corresponding authors.

13 E-mail: liucheng@suda.edu.cn Tel: (86)-0512-65882037

14 Email: whning@suda.edu.cn Tel: (86)-0512-65882037

15 E-mail: yyli@suda.edu.cn Tel: (86)-0512-65882037

16

17 **Quantitative Analysis of Bonding Interactions via COHP**

18 In this study, the Crystal Orbital Hamilton Population (COHP) analysis was
19 employed to gain insights into the nature of interatomic interactions within the material.
20 COHP offers a quantitative means to assess the bonding or anti-bonding contributions
21 of chemical bonds.¹ By projecting the expectation values of the Hamiltonian operator
22 onto the orbitals of specific atom pairs, COHP analysis reveals the distribution of
23 bonding and anti-bonding states at various energy levels.

24 Specifically, COHP is achieved by analyzing the orbital information obtained
25 from electronic structure calculations, such as those based on Density Functional
26 Theory. The COHP for each pair of atoms can be expressed as:

$$27 \text{COHP}_{ij}(E) = - \sum_k P_{ij}^k H_{ij}^k \delta(E - E_k)$$

28 Where P_{ij}^k and H_{ij}^k represent the crystal orbital overlap and Hamiltonian matrix
29 elements, respectively, and E_k is the corresponding eigenvalue of energy. The
30 integrated COHP (ICOHP) values quantify the total bonding and anti-bonding
31 contributions over the entire energy range.

32 ***d*-band Center Calculation for Transition Metals**

33 In the present investigation, particular attention was devoted to the position of the
34 *d*-band center of transition metal surfaces, a key factor in understanding their catalytic
35 activities. The *d*-band center refers to the weighted average energy position of the *d*-
36 state electrons in transition metals, significantly influencing surface adsorption
37 properties and catalytic reactions. According to the theory proposed by Hammer and
38 Nørskov, the position of the *d*-band center is intimately related to the electronic
39 structure of adsorption sites on the catalyst surface.²

40 The location of the *d*-band center is determined by calculating the energy-weighted
41 average of the *d*-electron states density on the surface. The calculation formula is as
42 follows:

$$\epsilon_d = \frac{\int \epsilon D_d(\epsilon) d\epsilon}{\int D_d(\epsilon) d\epsilon}$$

44 where ϵ represents the energy and $D_d(\epsilon)$ is the density of states function for the d -
 45 states. The energetic proximity of the d -band center to the Fermi level dictates the
 46 strength of the interaction between the metal surface and the adsorbed molecules.
 47 Typically, the closer the d -band center is to the Fermi level, the stronger the interaction
 48 with the adsorbate.

49
 50
 51

52 **Table S1** Free energy of TM-BTA with the adsorption of *OOH.

Type	E _{total} (eV)	G _{corr} (eV)	G _{total} (eV)
Sc	-253.204	0.329	-252.875
Ti	-254.842	0.384	-254.458
V	-254.860	0.363	-254.498
Cr	-255.011	0.319	-254.692
Mn	-253.387	0.334	-253.053
Fe	-250.774	0.333	-250.441
Co	-247.827	0.321	-247.506
Ni	-244.173	0.288	-243.886
Ru	-250.657	0.292	-250.365
Rh	-247.091	0.336	-246.760
Pd	-242.430	0.252	-242.178
Pt	-245.020	0.257	-244.763

53

54 **Table S2** Values of d -Band Centers for Co-BTA and Rh-BTA under varied strain
 55 conditions.

Strain	-1.95%	-1.30%	-0.65%	0.00%	+0.65%	+1.30%	+1.95%

Co	-1.846	-1.775	-1.789	-1.746	-1.783	-1.743	-1.735
Rh	-1.713	-1.606	-1.538	-1.457	-1.509	-1.457	-1.464

56

57 **Table S3** Under different strain conditions, the average bond length (Å) between the
58 metal center atom and the surrounding coordination atoms before and after *OOH
59 adsorption.

Type	-1.95%	-1.30%	-0.65%	0.0%	+0.65%	+1.30%	+1.95%
Sc	N-M	2.092	2.101	2.113	2.121	2.128	2.141
	N- M(*OOH)	2.204	2.210	2.209	2.237	2.227	2.234
Ti	N-M	2.003	1.982	1.989	1.996	2.004	2.044
	N- M(*OOH)	2.049	2.044	2.039	2.047	2.043	2.055
Cr	N-M	1.942	1.968	1.981	1.993	2.007	2.020
	N- M(*OOH)	1.967	1.981	1.981	1.987	2.007	2.019
Mn	N-M	1.894	1.903	1.912	1.920	1.928	1.939
	N- M(*OOH)	1.925	1.923	1.928	1.935	1.944	1.953
Fe	N-M	1.847	1.861	1.872	1.879	1.887	1.899
	N- M(*OOH)	1.892	1.890	1.892	1.898	1.907	1.918
Co	N-M	1.819	1.827	1.836	1.845	1.855	1.865
	N- M(*OOH)	1.866	1.867	1.867	1.872	1.881	1.892
Ni	N-M	1.822	1.830	1.841	1.849	1.858	1.868
	N- M(*OOH)	1.837	1.845	1.855	1.865	1.874	1.885
Rh	N-M	1.945	1.953	1.966	1.973	1.985	1.996
	N- M(*OOH)	1.992	1.991	1.991	1.997	2.008	2.025
Pd	N-M	1.965	1.974	1.985	1.994	2.002	2.013
	N- M(*OOH)	1.969	1.978	1.988	1.999	2.009	2.021
Pt	N-M	1.968	1.976	1.987	1.994	2.002	2.013
	N- M(*OOH)	1.977	1.982	1.990	1.999	2.010	2.019

60

61 **Table S4.** The calculated formation energies (ΔE_{form}) of Ni-, Co-, and Rh-BTA.

Type	Ni-BTA	Co-BTA	Rh-BTA
ΔE_{form} (eV)	-4.246	-4.956	-4.478

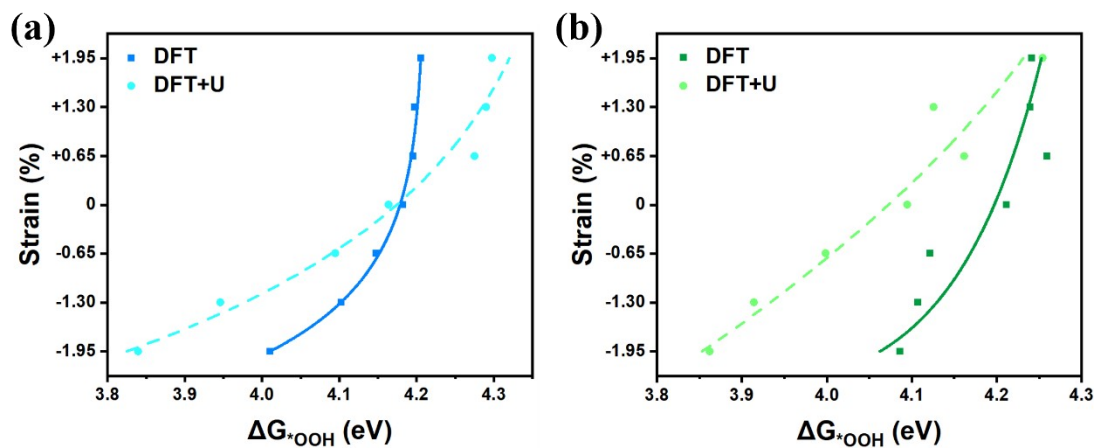
62

63 The corresponding formation energy calculation formula is stated as follows:

$$\Delta E_{\text{form}} = E_{\text{TM-BTA}} - E_{\text{BTA}} + 2E_{\text{H}_2} - \mu_{\text{TM}}^0$$

64

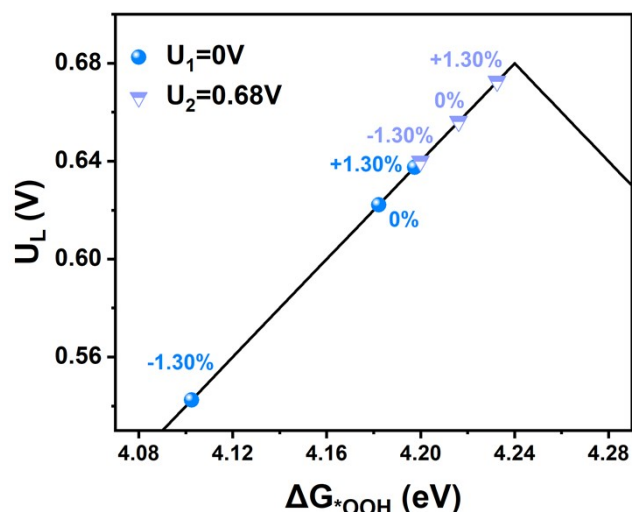
65



66

67 **Fig. S1.** Plot of the relationship between ΔG^*_{OOH} values and the dependent variable
68 obtained by studying the DFT and DFT+U methods, (a) Co-BTA, (b) Rh-BTA. In view
69 of the fact that Co and Rh are elements of the same main group and have similar
70 properties, the same U value of 3.42 eV was used for correction, and the corresponding
71 U value was taken from Reference 3.

72



73

74 **Fig. S2.** Trend of the limiting potential of Co-BTA as a function of strain at different
 75 electrode potentials.

76

77 **Modeling Structure:**

78 The structural model consists of two consecutive units in the long chain of TM-
 79 BTA, containing 8 nitrogen (N) atoms, 12 carbon (C) atoms, 2 transition metal (TM)
 80 atoms, and 12 (H) hydrogen atoms. To avert interlayer interactions stemming from the
 81 model's periodicity, a vacuum layer exceeding 15 Å was implemented. Due to the
 82 excessive length of the model structure information, we only present the detailed atomic
 83 coordinates of Co-BTA and Rh-BTA catalysts below, and the structures of other TM-
 84 BTA are consistent with the above two catalysts. The detailed atomic coordinates
 85 within the Co-BTA and Rh-BTA structures are presented as follows:

86

87 Co-BTA

88 1.0000000000000000

89 15.3491017285728528 0.0000000000000000 0.0000000000000000

90 0.0000000000000000 15.0000000000000000 0.0000000000000000

91 0.0000000000000000 0.0000000000000000 15.0000000000000000

92 N C Co H

93 8 12 2 12

94	Direct			
95	0.0895902379050250	0.4991186746333861	0.3865148392397993	
96	0.0895887834221885	0.5012397328976045	0.5498835635452040	
97	0.4098006943556209	0.4982958718898646	0.3865262809346313	
98	0.4098001216528388	0.5004129707827337	0.5498950532058443	
99	0.5895902069050261	0.4991186746333861	0.3865148392397993	
100	0.5895887444221890	0.5012397328976045	0.5498835635452040	
101	0.9098007253556267	0.4982958718898646	0.3865262809346313	
102	0.9098000596528411	0.5004129707827337	0.5498950532058443	
103	0.1711729500927192	0.5004863898511075	0.5173103360165816	
104	0.2496951073533480	0.4983585636293733	0.3716685678086143	
105	0.1711732738492757	0.4992387175269557	0.4191008214195861	
106	0.2496928267641682	0.5007742693669117	0.5647549011889900	
107	0.3282155322063594	0.5000712635554716	0.5173169629724071	
108	0.3282172100167997	0.4988248276336688	0.4191075844708111	
109	0.6711729500927193	0.5004863898511075	0.5173103360165816	
110	0.7496950913533464	0.4983585636293733	0.3716685678086143	
111	0.6711732738492757	0.4992387175269557	0.4191008214195861	
112	0.7496927947641655	0.5007742693669117	0.5647549011889900	
113	0.8282155322063595	0.5000712635554716	0.5173169629724071	
114	0.8282172100167997	0.4988248276336688	0.4191075844708111	
115	0.4996944040707945	0.4998016422790791	0.4682057959301015	
116	0.9996943720707989	0.4998016422790791	0.4682057959301015	
117	0.0851034233706787	0.4985115789467765	0.3185155831273289	
118	0.0850903367907922	0.5024101604251938	0.6178757992400530	
119	0.2496934025220973	0.4973564361431386	0.2988732091262277	
120	0.2496922799568755	0.5015350026233641	0.6375557946369916	
121	0.4142919573684221	0.4972492176786306	0.3185323861921964	
122	0.4142925183019936	0.5011376571367452	0.6178934149446138	
123	0.5851034543706779	0.4985115789467765	0.3185155831273289	

124	0.5850903677907910	0.5024101604251938	0.6178757992400530	
125	0.7496934025220974	0.4973564361431386	0.2988732091262277	
126	0.7496922479568729	0.5015350026233641	0.6375557946369916	
127	0.9142918953684170	0.4972492176786306	0.3185323861921964	
128	0.9142925803019987	0.5011376571367452	0.6178934149446138	
129				
130				
131				
132	Rh-BTA			
133	1.0000000000000000			
134	15.8723944742817356	0.0000000000000000	0.0000000000000000	
135	0.0000000000000000	15.0000000000000000	0.0000000000000000	
136	0.0000000000000000	0.0000000000000000	15.0000000000000000	
137	N	C	Rh	H
138	8	12	2	12
139	Direct			
140	0.0954818285310498	0.4991080770760946	0.3844900472014136	
141	0.0954781254528985	0.5012766839198949	0.5519068476612741	
142	0.4039118509360499	0.4982466549370634	0.3845020481363073	
143	0.4039127928193034	0.5004123177241165	0.5519197348671527	
144	0.5954817975310507	0.4991080770760946	0.3844900472014136	
145	0.5954780864528990	0.5012766839198949	0.5519068476612741	
146	0.9039118819360560	0.4982466549370634	0.3845020481363073	
147	0.9039127308193053	0.5004123177241165	0.5519197348671527	
148	0.1735333118752028	0.5005044316520921	0.5174143176071638	
149	0.2496950440494412	0.4983701250801783	0.3719950909446707	
150	0.1735339421626845	0.4992518411569508	0.4190007811293734	
151	0.2496940220437394	0.5007827031942313	0.5644293280674303	
152	0.3258565912512599	0.5000698454373815	0.5174196332427976	
153	0.3258572071023307	0.4988184955120521	0.4190057418785815	

154	0.6735333118752029	0.5005044316520921	0.5174143176071638
155	0.7496950280494399	0.4983701250801783	0.3719950909446707
156	0.6735339421626845	0.4992518411569508	0.4190007811293734
157	0.7496939900437365	0.5007827031942313	0.5644293280674303
158	0.8258565912512602	0.5000698454373815	0.5174196332427976
159	0.8258572071023306	0.4988184955120521	0.4190057418785815
160	0.4996963121292030	0.4997956539071644	0.4682030661506385
161	0.9996962801292073	0.4997956539071644	0.4682030661506385
162	0.0935242602477702	0.4985199849757916	0.3163298219316670
163	0.0935111106643159	0.5024709240852789	0.6200590122280992
164	0.2496911484120483	0.4973632388197735	0.2991515852694218
165	0.2496903188952541	0.5015425345903327	0.6372766798046936
166	0.4058683034479623	0.4971741864837921	0.3163477184545144
167	0.4058688899794836	0.5011152784478171	0.6200794394247835
168	0.5935242912477693	0.4985199849757916	0.3163298219316670
169	0.5935111416643151	0.5024709240852789	0.6200590122280992
170	0.7496911484120484	0.4973632388197735	0.2991515852694218
171	0.7496902868952516	0.5015425345903327	0.6372766798046936
172	0.9058682414479571	0.4971741864837921	0.3163477184545144
173	0.9058689519794887	0.5011152784478171	0.6200794394247835
174			

175 **References**

- 176 1. R. Dronskowski and P. E. Bloechl, *The Journal of Physical Chemistry*, 1993, **97**, 8617-8624.
- 177 2. B. Hammer and J. K. Norskov, *Nature*, 1995, **376**, 238-240.
- 178 3. H. Xu, D. Cheng, D. Cao and X. C. Zeng, *Nature Catalysis*, 2024, **7**, 207-218.
- 179